Sensitivity Analysis of Aerodynamic Performance of Airfoils Used in Small Wind Turbines

Jorge Antonio Villar Alé
Ricardo Schuh Frantz
Felipe Weigel
PUCRS University – Brazil
villar@pucrs.br

António Manuel Gameiro Lopes
Coimbra University – Portugal
antonio.gameiro@dem.uc.pt

Svend Enevoldsen
HS Wind Randers – Denmark
svend@ecology.dk

Abstract

This paper applies a blade element theory code to predict the performance on a stall-regulated small wind turbine. A partnership with a wind turbine manufacturer allowed to know the blade geometry and experimental results power curve. The WT_Perf code was used with a three-bladed rotor using the same airfoil along the blade. With use of XFLR5 and EasyCFD codes were obtained the aerodynamic coefficients of lift and drag for different angle of attack. Later a AirfoilPre spreadsheet is used to extension these coefficients for higher angles of attack. The paper also included an analysis of stall delay models. The results compare the BEM code predictions with the manufacturer power curve. Several tests were performed considering: (i) a sensitivity analysis of the polar data from experimental and computational source. (ii) a sensitivity of results using different thickness airfoils. (iii) The stall delay models influence.

1. Introduction

The aerodynamic design of small wind turbines can be developed using computational tools based on the theory of momentum of the blade element (BEM) **[1].** Several applications such as PROPRID **[2],** WT_PERF **[3],** BLADED **[4]** use this theory. This methodology allows, through an iterative process, evaluating the interference factors axial and tangential velocity incident on a blade element. The identification of these factors subsequently allows the determination of elemental forces and the integration along the blade enables these forces determine the performance of the wind turbine featuring its power, torque and thrust coefficient. Such applications have subroutines which must be inserted in semi-empirical models taking into account effects of blade tip losses, 3D effects, stall dynamic effects as well as tower wake. In addition, applications must rely on tabular data of lift and drag coefficients (C_L and C_D) airfoil used. These data can be determined from references obtained experimentally in wind tunnel test. One of the difficulties is that often these results correspond to a Reynolds number much higher than those found in the blades of small wind turbines. When no account with this information, there are 3 alternatives for solving this problem:

(1) Experimental data from wind tunnel.
(2) Use codes with potential-viscous models.
(3) Using CFD codes (Navier-Stokes equations).

The first alternative has been a concern of several research laboratories conducted tests in the wind tunnel for airfoils at low Reynolds number, however with limited angles of attack the region near the dynamic stall. This alternative consumes more time and higher costs for its realization. The second option allows obtain the aerodynamic coefficients for the Reynolds number desired by computer codes using the panel method (potential flow) coupled with boundary layer equations, such as codes XFOIL **[5],** XFLR5 **[6].** These codes achieve quality results for low angle of attack. Thus the results should be processed to get tabular results of lift and drag with higher angles of attack. To achieve this are used Viterna and Corrigan **[7].** The application AirfoilPrep **[8]** is used for this purpose. Finally can be adopted as the commercial CFD codes FLUENT **[9],** CFX **[10],** CFD-RC **[11],** EasyCFD_G **[12]** which use the equations RANS (Reynolds Average Navier-Stokes), with equations for modeling specific turbulence, such as k-ε and k-ω. One of the difficulties of these models is able to predict the separation of the boundary layer especially for airfoils that operate with low Reynolds number. The results directly affect the lift and drag of the airfoil and make a significant difference computational result (BEM) which describes the aerodynamic performance of wind turbines. Some authors have drawn attention to weaknesses in these results **[13].**

2. General information

On the market, there are some small wind turbines designed with proper airfoils for low Reynolds number, thus allowing a rotor speed control by stall. A partnership with a wind turbine manufacturer allowed to know the type of airfoil used, besides the experimental results of a wind turbine power curve. Based on the geometric and operation data, it was possible to run the code WT_Perf and perform a sensitivity study of the aerodynamic coefficients with a similar thickness airfoil compared to the one used by the manufacturer. The paper presents an aerodynamic analysis of this wind turbine.

2.1 Turbine performance

This paper shows a comparative between original manufacturer power curve and WT_Perf results. **Fig. 1** shows the small turbine 25 kW and **Table 1** shows the main specification of this turbine. **Fig. 2** shows the power curve supplied by the manufacturer as well as the results obtained in tests performed in the field. The study was conducted with this machine for ease of information provided by the manufacturer. It is a stall-regulated turbine rotor whose blade has a design that uses a single airfoil, making it easier implementation and computational analysis of the results.

Figure 1: Three blade wind turbine

Table 1: Wind turbine specifications

Number of blade	3
Rotor diameter	13 m
Rated power	25 kW
Hub height	18 m
Power regulation	Stall
Cut-in wind speed	4,0 m/s
Rated wind speed	12 m/s
Cut-out wind speed	> 25 m/s
Rated power rotation	65 rpm

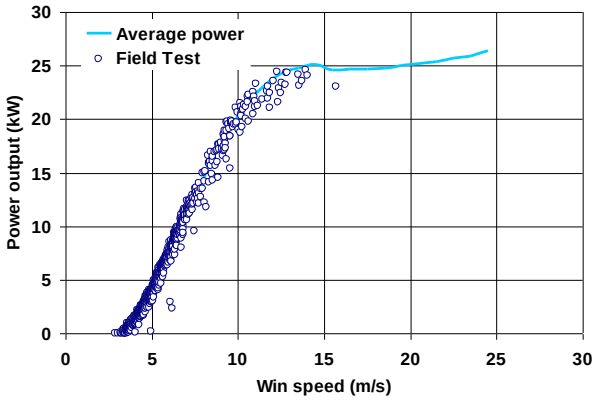

Figure 2: Power curve 25 kW wind turbine

2.2 Blade specifications

The twist and chord blade have a fit based on original manufacturer data, as seen in **Fig. 3**.

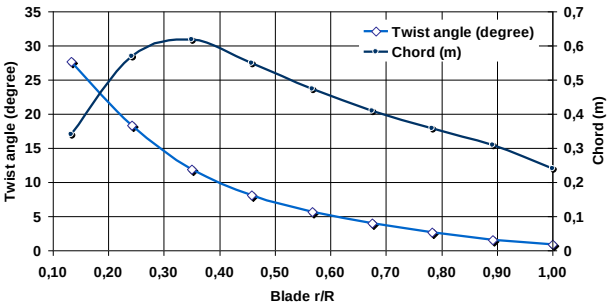

Figure 3: Twist angle and chord 25 kW turbine

3. Airfoils and codes design

The manufacturer uses blade airfoil thickness 15% whose design follows geometry of airfoil 14% thickness (Risø E1-14) projected by Risø laboratory. We rescaled the 14% to 15% thickness as seen in **Fig.4** being named in this work as E1-15. There are no experimental data for E1-15 airfoil for this we use the wind tunnel data from Risø E1-14. This airfoil was for use on the outerpart of blades for stall regulated wind turbines with a Reynolds number between one and two million **[27].**

Figure 4: Airfoil 15% thickness

3.1 Results using XFLR5

The first tool used is the XFLR5 code **[6]**. This one is an analysis tool for airfoils, wings and planes operating at low Reynolds Numbers. XFoil **[5]** is a code developed for accurately approximating the

flow over 2D and 3D airfoils, wings. XFLR5 **[6]** is a code that uses the XFoil solver with user-friendly interface. The algorithms for foil analysis implemented in XFLR5 are exactly the same as those of the original XFoil code, except for the translation from FORTRAN to C. The code include XFoil's direct and inverse analysis capabilities wing design and analysis capabilities based on the Lifiting Line Theory, on the Vortex Lattice Method, and on a 3D Panel Method. We computed airfoil Risø E1-14 polar curves on XFLR5 to Re=1,6 x10^6 using free transition (N_{Crit}=9) and compared with XFOIL. The results of XFOIL are not shown since they are very similar to those obtained in XFLR5. Furthermore, we used the XFLR5 and EasyCFD_G code to get the polar curves of 15% thickness airfoil.

3.2 Results using EasyCFD_G

The software EasyCFD_G **[12]** takes the Navier-Stokes equations in their incompressible 2D formulation. For modeling turbulence effects upon the mean flow field, the standard k-ε **[14]** and the SST k-ω **[15]** turbulence modes are available. The governing equations are discretized and integrated in a non-structured quadrilateral mesh generated with a paving technique similar to the proposal of **[16]**. Pressure and momentum are linked with SIMPLEC algorithm **[17].** The Rie-Chow interpolation procedure **[18]** is used to handle the collocated mesh arrangement. In order to improve converge behaviour and reduce calculation time, a multigrid method is adopted for the global solution, while the pressure correction equation is solver using an additive correction strategy. The **Fig. 5** shows the generated mesh with EasyCFD. This is an unstructured mesh with 60000 elements It was created with a domain having a about 10 chords far of airfoil.

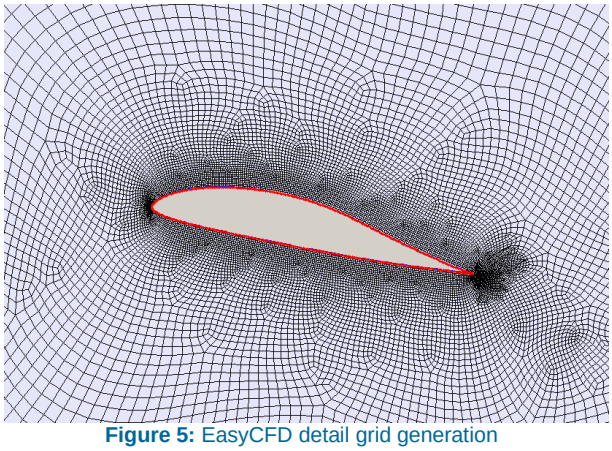

Figure 5: EasyCFD detail grid generation

3.3 Comparative airfoils lifts

Fig. 6 shows the set of results to determine the aerodynamic coefficient at angles between -10 and 20 degrees. The XFLR5 allowed to determine the airfoil aerodynamic coefficients of thickness of 14% and 15%. The EasyCFD_G was used to determine the aerodynamic coefficients of 15% airfoil to Re=1.0x10^6. In the same figure (**Fig. 6)** are presented the experimental data of airfoil 14% provided by the manufacturer and airfoil 18% data to Re=1,6x10^6 from **[26]**.

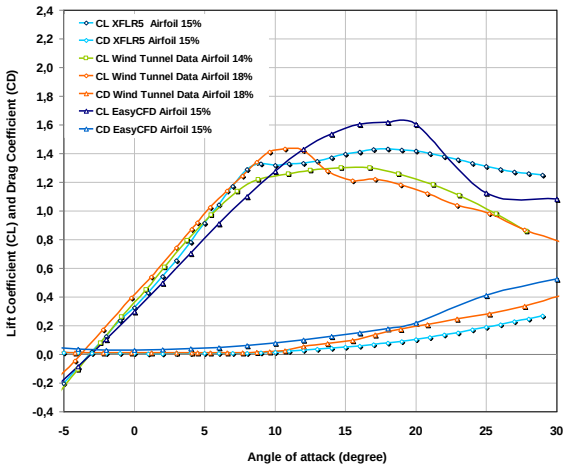

Figure 6: Lift coefficient airfoil 15%

3.4 Extrapolation airfoil data

In order to run tests in WT_Perf code **[3],** these data are extended using the AirfoilPrep **[19].** AirfoilPrep is a NREL spreadsheet that helps generate airfoil data files needed by WT_Perf an Aerodyn codes. From a series of data with limited angle of attack, the tool uses the Viterna and Corrigan model to expand ±180^0. The tool can interpolate the aerodynamic coefficients for other span locations. It can also apply rotational augmentation corrections for 3-D stall delay.

The results are shown in **Fig. 7** the lift coefficient obtained by codes and experimental data reference, using aspect ratio AR=20. It is observed the divergence of C_L results in the pos stall region.

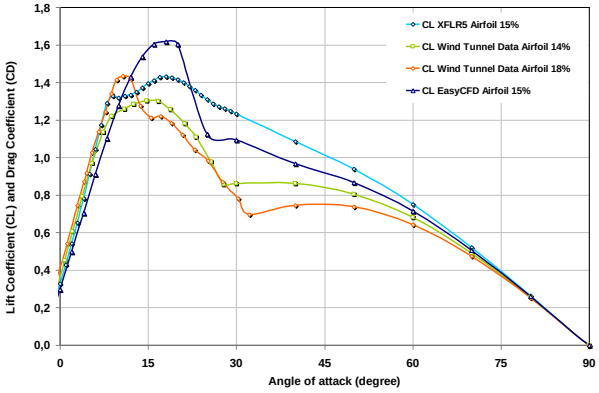

Figure 7: Lift coefficient extension

4. BEM Tool

There are many applications for computational aerodynamic design of wind turbines. This work use the WT_Perf code provided by the National Centre for Technology Wind Turbines U.S. (NWTC) that is part of NREL (National Renewable Energy Centre). The tool uses the blade element theory (BEM) allows evaluate the performance of wind turbines. The code is a descendant of PROP, developed at Oregon State University in the Seventies with theoretical found in Wilson and Walker **[20].** The WT_Perf uses as basis algorithms PROP-PC code **[21].** NWTC staff rewrote and improved the program and provides the application, along with a user guide **[3].** The application is written in Fortran performs an analysis of a rotor in steady state. The user defines the geometry of the rotor length and angle of twist of the blade airfoil type used in the blade section, as well as speed and rotation operation. The results allow to determine the rotor power coefficient, power, torque as well as the details of aerodynamic forces along the blade. **Fig.8** shows the structure of a program that provides main file with all input data required for assessing the performance of a wind rotor. After using the file input the code executes the program which allows the numerical solution of the models used, which is based on the theory element shovel or BEM (Blade Element Momentum theory). Finally the program generates two files with the main results.

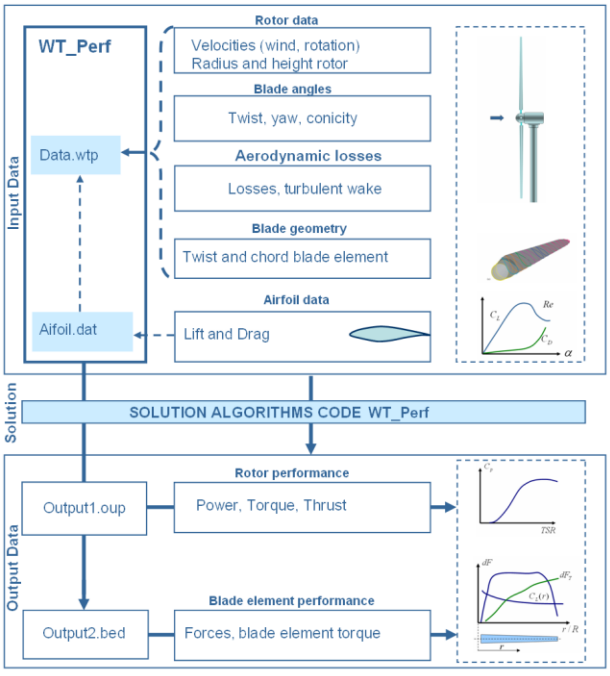

Figure 8: WT_Perf code structure

4.1 BEM Preliminary Results

The results include the power coefficient and power curve. For the determination of the coefficients C_L and C_D were used following:

(a) (C_L,C_D) from XFLR5.
(b) (C_L,C_D) from EasyCFD_G
(c) (C_L,C_D) from reference wind tunnel data.

In all cases was used AirfoilPre to perform an extension of the airfoil tabular data for larger angles of attack used Viterna and Corrigan corrections. The **Fig.9** shows the power curve using airfoil 14%, 15% and 18% thickness. The C_L and C_D data were obtained from XFLR5 and the extrapolation using Viterna and Corrigan model. There is a great divergence of results, compared manufacturer power curve. The **Fig.9** also shows the result of power curve using experimental data of the 14% and 18% thickness and extent of the data using the Viterna and Corrigan model. As noted the WT_Perf code shows an overall sensitivity of the results to the values of lift and drag of the post stall region. Considering the result of the airfoil 14% using C_L and C_D from XFLR5 and experimental data is observed have a drastic drop in power between 13 m/s to 25 m/s that is directly related to aerodynamic curve in the region of pos stall (see **Fig.7**).

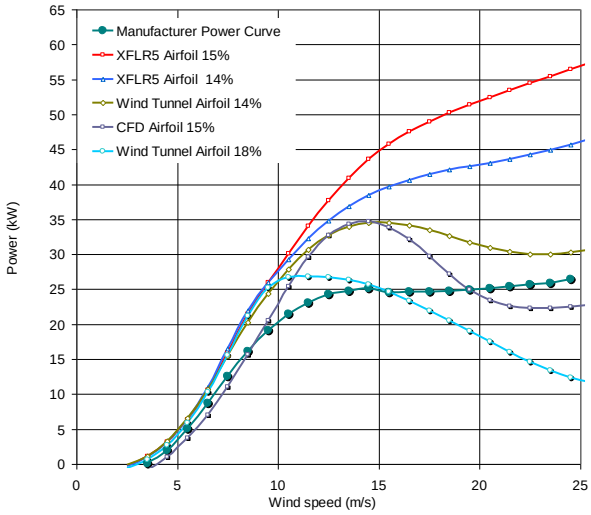

Figure 9: Power curve results

The **Fig. 9** shows that the best results are obtained using the C_L and C_D coefficients determined in the wind tunnel and extended by Viterna and Corrigan model. So far the tabular data were obtained with XFLR5 and EasyCFD code and extended with Viterna Corrigan corrections but not yet included 3D post stall corrections. In the following sections will be covered such models and their effects on the code used.

4.2 BEM and Stall Delay Corrections

The phenomenon of stall delay occurs on the blades of wind turbines causing a lift aerodynamic (3D) with magnitude greater than found in the data collected in the wind tunnel (2D). The phenomenon occurs sharply in sections of the blade closest to the rotor hub, reducing the effect towards the tips of the blades. It is a complex phenomenon not yet fully understood, however it is recognized that is mainly due to centrifugal force and Coriolis force. The centrifugal force creates a movement of fluid toward the tips of the blades while the Coriolis force causes an acceleration of the fluid leading edge to the trailing edge. As a result the pressure gradient becomes less adverse delaying boundary layer separation. This delay separation allows for large angle of attack, an increase in aerodynamic lift.

Two projects conducted in wind tunnel were fundamental to study the aerodynamics of rotors not stationary wind turbine: The MEXICO and UAE Phase VI and experiments **[22].** These experiments were very important to better understand the stall delay on rotors of wind turbines in operation.

4.3 Stall Delay Models

Several semi-empirical or engineering models have been used to approach modeling the aerodynamic forces in the BEM models of wind turbines. Brenton **[23]** presented a study with different models available stall delay compared with the experiment of NREL UAE Phase VI. The author observed that these models have different results and it is not conclusive which model is most appropriate. The IEA's report **[24]** also provides comparative results of stall delay and CFD models using experiment results of NREL UAE Phase VI. According to the report, the stall delay models appear far from satisfactory. These models require adjustment of the coefficients and constants used to improve results, but the result depends on the case to be applied. The report indicates that results using CFD codes are better and should be preferred.

Most models stall delay presents a similarly given by:

$$C_{L3D} = C_{L2D} + f_L \Delta C_L \quad (1)$$

$$\Delta C_L = C_{L,linear} - C_{L2D} \quad (2)$$

The term $C_{L,linear}$ represents the linear coefficient. The f_L coefficient depends mainly on the ratio (c / r) of the blade element analysis. The models may have a similar equation for the drag coefficient, changing the constants used.

$$C_{D3D} = C_{D2D} + f_D \Delta C_D \quad (3)$$

$$\Delta C_D = C_{D,linear} - C_{D2D} \quad (4)$$

In this paper are presented results using 6 stall delay models:

- Snel model
- Linderburg model
- Du and Selig model
- Dumitrisco and Cardos model
- Corrigan e Schillings model
- Chaviaropoulos and Hansen model

These models can be found in reference **[23]** and **[24].** The model Dumitrescu and Crados found in reference **[25].** The results are limited to show the behavior of the models for the lift coefficient to specific airfoil. **Fig. 10** shows the results using as reference 2D wind tunnel data of airfoil RISO 18% to Re=1,6x10^6. The models were evaluated for the rotor with $r/R=0.32$ and $c/r=0.30$. The Snel and Linderburg model show similar results. The Du and Selig model is closer to Dumitriscu Cardos model. The Corrigan and Schillings model provides different results since the base of this model is also different. In addition this model also makes a correction to the angle of attack.

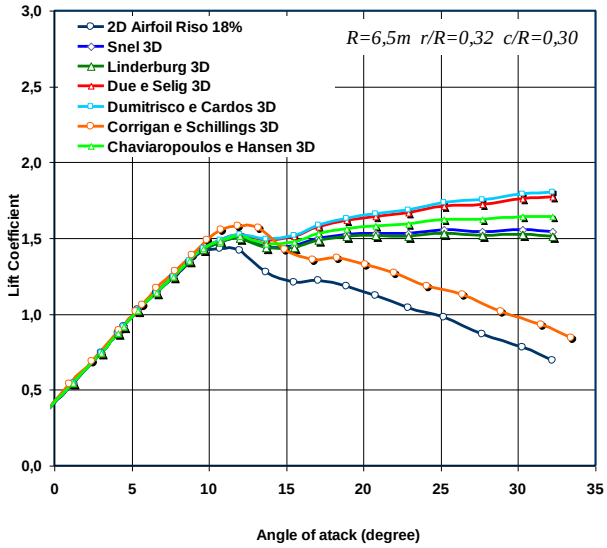

Figure 10: Power curve results

4.4 Stall Delay Model Results

The AirfoilPre tool uses the Du and Selig stall delay model. For lift and drag data including the effect of delay stall along the rotor blade was used HARP_Opt code. This code allows to generate with better quality a series of tables (3D_Airfoil_Data) using the Du and Selig model. As the drag decreases in this model, the code can use the Eggers model allowing an increased in the drag. This code was developed for the NREL performance optimization of wind turbine rotors, using genetic algorithms and WT_Perf. In the present work was not carried out a detailed study of the code. However, it was possible to obtain an optimized geometry of the rotor of the wind turbine studied.

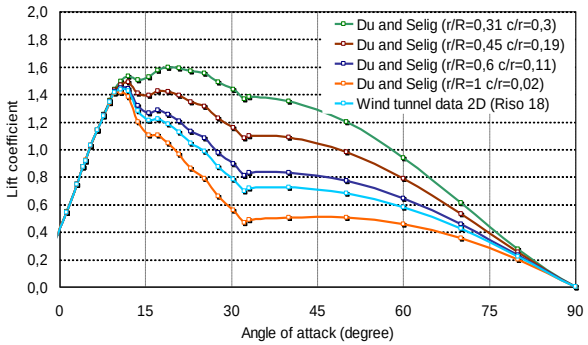

Figure 11: 3D interpolation using HARP_Opt.

The **Fig. 11** shows the result of extrapolation of the aerodynamic lift including 3D effects. As noted in sections of the rotor blade near the 3D effect is most pronounced. These files were generated by HARP_Opt in WT_Perf used to check the behavior of the rotor with an optimized geometry. The **Fig. 12** shows the original manufacturer blade geometry and the geometry obtained by HARP_Opt. The result of the optimization (**Fig.12**) presents a blade chord distribution very similar to the manufacturers, however, a different twist angle.

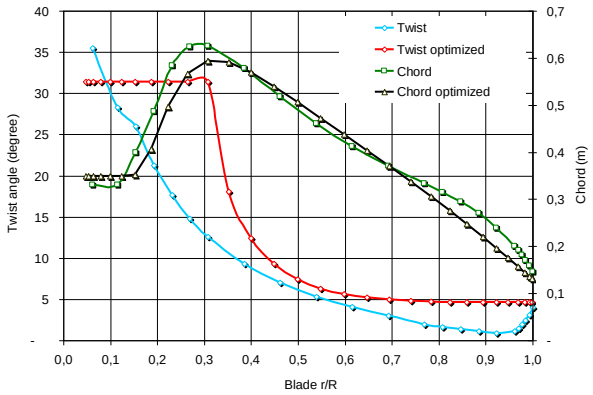

Figure 12: Optimization geometry using HARP_Opt.

The **Fig.13** shows the power curve results using the same airfoil with and without stall delay model.

In the first case the 14% airfoil were used along the blade with 30 elements twist and chord equally spaced and only one data file with C_L and C_D uncorrected 3D effects. In the pre-stall region were used wind tunnel data from airfoil 14%. In the pos stall region is used Viterna and Corrigan model. In the second case the airfoil of 14% were used with 30 elements (twist and chord) along the blade and a battery of C_L and C_D files generated by HARP_Opt including 3D corrections Du and Selig model and in the pos stall a Viterna and Corrigan model. It is observed that the delay stall model causes an increase in the power curve. If assumes that if we apply the method of 3D stall for the other cases shown in **Fig. 9** results are further away from the manufacturer curve.

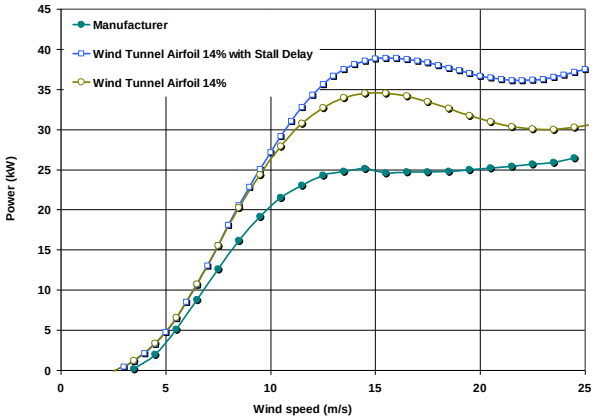

Figure 13: Power results using 3D corrections

It should be noted that the coefficient of power manufacturer takes into account all the losses since the system is obtained using the electrical power of the machine. An example of the result of the power coefficient compared with the power coefficient manufacturer is shown in **Fig.14.** In the present study, we conducted an approximation that allows to take into account this difference to correct the results obtained by WT_Perf;

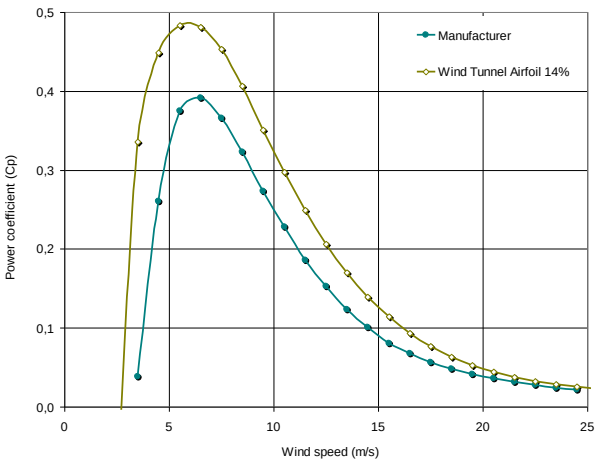

Figure 14: Power coefficient results.

4.5 Estimated losses generator

So far we compared the results of power curves model and the power curve obtained from the manufacturer in the field. The BEM code does not take into account the losses of mechanical transmission and electric generator. To counter this we performed a procedure that allows us to estimate the efficiency of the system. We compared the results of all power coefficients obtained in computer simulations with the coefficient of power supplied by the manufacturer. A simple division between them for the entire power range that operates the machine gives us a curve of average efficiency of the system. This curve is shown in **Fig. 15**.

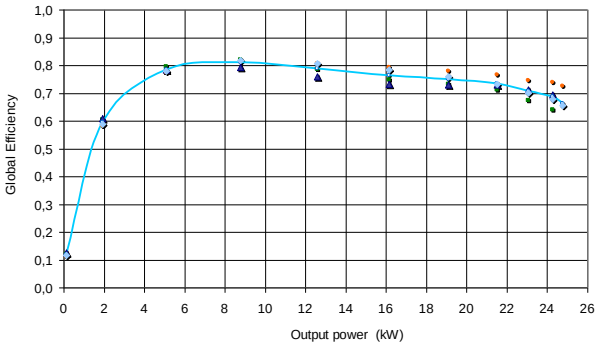

Figure 15: Global efficiency estimative

An adjustment of the above equation gives the following expression:

$$\eta_{sis} = \frac{A + B\dot{W}_{BEM}}{1 + C\dot{W}_{BEM} + D\dot{W}_{BEM}^2} \quad (5)$$

Were $\dot{W}_{BEM}$ is the power obtained using the BEM code and A,B,C,D are constants approximating the curve of efficiency, provided in the **Table 2**.

Table 1: Equations constants

A	0,048
B	0,615
C	0,534
D	0,013

Finally $\dot{W}_{Elec}$ Is determined considering this efficiency.

$$\dot{W}_{Elec} = \eta_{sis}\dot{W}_{BEM} \quad (6)$$

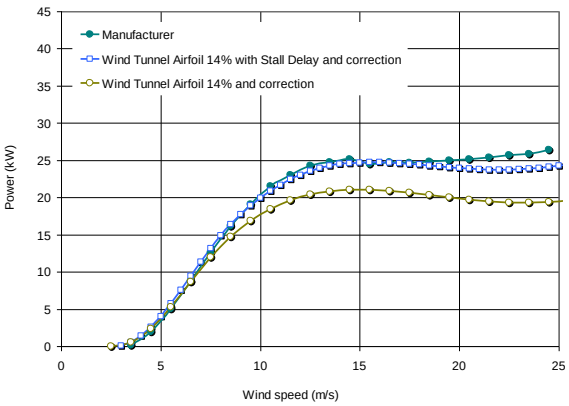

Figure 16: Generator efficiency estimation

Using this approach **Fig. 16** show the results. Observed that when not considering stall delay effect results underestimates the power curve. It is noted that the results becomes very promising considering the effect of stall delay and efficiency correction. However, it should be noted that it was only possible to reach this results knowing the actual performance of the machine. Otherwise, the results obtained with the BEM model, even with all settings and stall delay models show results that overestimates the power curve. The **Fig. 16** also shows that the curve obtained with the method provides lower power values than the manufacturer for speeds higher than 15 m/s. There is difficulty interpreting the deviations of the power curve for wind speeds above 15 m/s since very few field data obtained by the manufacturer that exceed this value. This can be observed (**Fig.17)** in raw data of wind turbine power curve obtained in the field by the manufacturer.

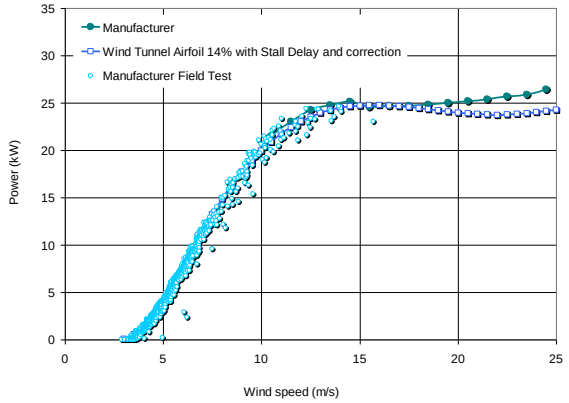

Figure 17: Generator efficiency estimation

5. Operations Envelope

The wind turbine may operate at a level of 4.0 to 25 m/s. The **Figure 18** shows the envelope of operation of the Reynolds number for different radial positions and for different wind speeds. It is observed that the Re of the turbine does not exceed $1.3x10^6$ and the airfoil data used correspond at Re=$1.6x10^6$ which may have influenced the results. At rated wind speed (V=12 m/s) the turbine operates with a blade Re≅$0.85x10^6$. Another important aspect related to the performance of the turbine is the angle of attack envelope in the blade. The **Fig. 19** shows that elements close to the hub of the rotor have an angle of attack between 4^0 and 40^0 whereas for elements near the blade tip have an angle of 4^0 to 30^0. Observing also **Fig. 7** and **Fig. 9** shows that the greatest differences result the power curve are present in the region with these angles of attack, where the aerodynamic lift coefficient has different values according to the method used (computational or experimental). This analysis shows the importance of quality polar data used and his influence in the power curve.

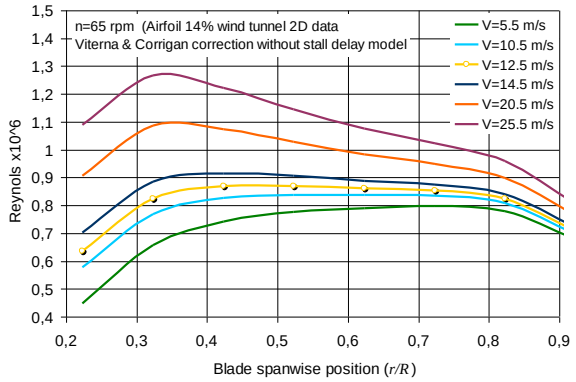

Figure 18: Reynolds envelope wind turbine

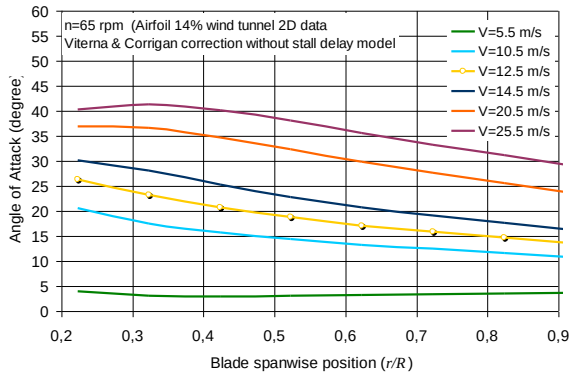

Figure 19: Angle of attack envelope wind turbine

6. Conclusions

At work a study was conducted to evaluate the aerodynamic performance of a small wind turbine. In the methodology were applied computer codes to determine aerodynamic characteristics of airfoils and turbine performance in terms of power curve of the turbine. One of the main interests in the study was to evaluate (i) the sensitivity of results with respect to the polar curves used for the same airfoils and obtained from airfoil design tools and experimental data. (ii) the sensitivity of results to airfoils of different thickness. (iii) stall delay models and your influence in the results. After tests can conclude the following:

(a) Tools airfoil design and analysis can be used to determine the aerodynamic coefficients, however, are critical regions such as the stall and post stall such tools quality can not describe the physical phenomena that occur in the airfoils primarily for high angles of attack. The results of the curves obtained with polar XFLR5 perform better than the results obtained with EasyCFD_G compared with experimental data.

(b) The results of this work show that the wind tunnel data of two-dimensional airfoils are still a quality base for use in BEM codes.

(c) For this work had not experimental data of 2D airfoil thickness of 15% used by the manufacturer. We used experimental data of other airfoils that are also suitable for stall regulated wind turbines. We use the data airfoil Riso E1-14 with (14% thick) and the airfoil Risø A1-18 (18% thick). The results presented show marked differences in terms of the power curve using polar data from this airfoils. The best performance was 14% of the airfoil which makes sense since the airfoil manufacturer was generated from this type of geometry. The results for the airfoil 15% using XFLR5 and Easy_CFD are not as suitable as the results obtained using experimental data from Risø E1-14.

(d) EasyCFD_G is a tool that allows quickly results however the results are conditional on the quality of the generated mesh. In addition it is important to verify that the turbulence models can effectively describe the physical phenomena especially in flows with boundary layer separation. This project is a partnership with the team EasyCFD_G to validate the tool for use in applications that enable the design of airfoils used in wind turbines.

(e) In this work observed that the most problematic region and significant divergence of results is found in the region of pos stall angle of attack to 20^0 to 60^0.

(f) The Du and Selig model applied in the work results in increased power curve. This result produces a greater divergence with the manufacturer's power curve and not a better approximation of the curve as expected. However, using the efficiency correction becomes the curve that best represents the power performance of the manufacturer.

(g) The paper proposes a method to consider the overall efficiency of the turbine related to theoretical BEM power curve with electric power curve of the manufacturer. The resulting equation allows a good approximation of the model with the curve of the manufacturer. However, it is necessary to have the experimental curve of the manufacturer. Thus it is a limitation when you want to design a wind turbine and not only the performance verification as was the case presented in this work. Otherwise, the results obtained with the BEM model, even with all the optimizations tend to overestimate the power curve.

There are many activities that can still be done in order to achieve a better quality of the methodology applied. For example one can use the six stall delay models presented in order to see their performance results in the power curve. Further tests with CFD tools to verify influence of Reynolds number in the results obtained. It would be interesting to validate the correction that allowed to determine the electrical power turbine, using the concept of overall system efficiency.

The work was a valuable learning regarding the potential of computational tools that can be used to evaluate the performance of small wind turbines as well as the care that must be taken to use the best possible way.

Acknowledgments

This work was supported by the project CNPq National Council for Scientific and Technological Development, Government of Brazil, Call MCT / CNPq No5/2010.

References

(1) Hansen M.O.L. Aerodynamics of Wind Turbines. Rotors, Load and Structures. James & James: London, 2000.
(2) Selig M. S., et al. PROPID User Manual. Aerodynamic Design Software for Horizontal Axis Wind Turbines Version 5.3.1. (2012) UIUC Applied Aerodynamics Group Department of Aerospace Engineering.
(3) Bulh, Jr., M.L., WT_PERF User´s Guide. , Last revised Dec, 17, 2004. Version 3.1.
(4) Bossanyi E.A. Bladed Theory Manual, GH & Parteners Ltd. 2003.
(5) Drela M.: Xfoil An Analysis and Design System for Low Reynolds Number Airfoils. Low Reynolds Number Aerodynamics, Springer-Verlag, Lec. Notes in Eng. 54, 1989.
(6) Deperrois A. User´s Manual, XFLR5 Analysis of Foils and Wings Operating at Low Reynolds numbers, (2009)
(7) Tangler J.; J. D. Kocurek Wind Turbine Post-Stall Airfoil Performance Characteristics Guidelines for Blade-Element Momentum Methods. NREL Report/CP-500-36900. Oct. 2004
(8) Marshall L. Buhl Jr. The NWTC Design-Codes Suite: An Overview . NREL-NWTC (2005)
(9) ANSYS Fluent software www.ansys.com
(10) ANSYS CFX software www.ansys.com
(11) CFD-RC software www.cfdrc.com
(12) Gameiro L. A. M. EasyCFD_G User Manual. (2012). www.easycfd.net
(13) Tangler J. L. The nebulous art of using wind-tunnel airfoil data for predicting rotor performance. NREL Report/CP-500-31243 (2002).
(14) Launder, B.E. and Spalding, D.B., Mathematical Models of Turbulence, Academic Press London and New York, ISBN 0-12-438050-6, 1972
(15) Menter, F.R. Zonal two-equation k-□ turbulence model for aerodynamic flows. AIAA Paper 1993-2906, 1993.

(16) Blacker, T.D. and Stephenson, M.B., "Paving: a New Approach to Automated Quadrilateral Mesh Generation", International Journal for Numerical Methods in Fluids, Vol. 32, pp. 811-847, 1991.

(17) Van Doormaal, J.P. and Raithby, G.D., "Enhancements of the Simple Method for Predicting Incompressible Fluid Flows", Numerical Heat Transfer, Vol. 7, pp. 147-163, 1984.

(18) Rhie, C.M. and Chow, W.L., "Numerical Study of the Turbulent Flow Past an Airfoil with

Trailing Edge Separation ", AIAA Journal, Vol. 21, N. 11, pp. 1525-1532, 1983.

(19) NWTC Design Codes (AirfoilPrep by Dr. Craig Hansen). http://wind.nrel.gov/designcodes/preprocessors/airfoilprep/. Last modified 28-June-2012; accessed 28-Nov-2012.

(20) Wilson, Robert E.; Walker, Stel N. Performance Analysis of Horizontal Axis Wind Turbines. Corvallis, OR: Oregon State University, September 1984. Prepared for the National Aeronautics and Space Administration Lewis Research Center under Grant NAG-3-278.

(21) Tangler, J.L. A Horizontal Axis Wind Turbine Performance Prediction Code for Personal Computers. An unpublished report. Golden, CO: Solar Energy Research Institute, January 1987

(22) Schreck S. Sant T. Micallef D. Rotational Augmentation Disparities in the MEXICO and UAE Phase VI Experiments. Conference Paper NREL/CP-500-47759 May 2010.

(23) Breton S.P. Study of the stall delay phenomenon and of wind turbine blade dynamics using numerical approaches and NREL's wind tunnel tests. Doctoral thesis, (NTNU) Norwegian University of Science and Technology (2008).

(24) Rooij, R.P.J.O.M. van. (2007). "Engineering Models vs. CFD Methods with Respect to Augmented Lift Caused by Blade Rotation." Proceedings of the 2007 Joint Meeting of IEA R&D Wind Annex XI: Joint Action on the Aerodynamics of Wind Turbines and IEA R&D Wind Annex XX: HAWT Aerodynamics and Models from Wind Tunnel Measurements, Roskilde, June 13–15, 2007. Golden, CO: NREL.

(25) Dumitrescu H. Cardos V. A stall-delay model for rotating blades Proc. Appl. Math. Mech. 7, 4100003–4100004 (2007) / DOI 10.1002/pamm.200700178

(26) Fuglsang, P.; Dahl, K.S.; Antoniou, I. / Wind tunnel tests of the Risø-A1-18, Risø-A1-21 and Risø-A1-24 airfoils. 1999. 101 p. (Denmark. Forskningscenter Risoe. Risoe-R; No. 1112(EN)).

(27) Madsen, H.A., (1994) Design of a 20 kW – 12.6 m stall regulated rotor. (In Danish) Risø-I-809(DA). Risø National Laboratory, Denmark.

(28) Fuglsang P., Ioannis A. Christian, B. Wind Tunnel Test of the RISØ-1 Airfoil (1998) Risø-R-999(EN).

(29) NWTC Design Codes (WT_Perf by Andrew Platt). http://wind.nrel.gov/designcodes/simulators/wtperf/. Last modified 26-November-2012; accessed 28-November-2012.